Production of high-coercivity materials based on $BaFe_{12}O_{19}$by crystallization of plasma-sputtered powders

A.A. Lepeshev[a,b*], I.V. Karpov[a,b], A.V. Uschakov[a,b]

[a] Krasnoyarsk Scientific Center of the Siberian Branch of the Russian Academy of Science, Krasnoyarsk 660036, Russia

[b] Siberian Federal University, Krasnoyarsk, 660041, Russia

* Corresponding author.

E-mail address: sfu-unesco@mail.ru (A.A. Lepeshev)

Abstract

Ferrite powders $BaFe_{12}O_{19}$ were studied in the present work after plasma heating and rapid quenching in differentenvironment: in air, in water and on the copper disk. X-ray diffraction analysis (XRD), scanning electron microscopy (SEM), vibration magnetometry (VSM) and Mossbauer spectroscopy (NGR) showed that the powder produced after quenching on the copper disk was in amorphous-crystalline state. The correlation between the annealing temperature and the value of magnetic parameters (coercive field and saturation magnetization) was established. Annealing at 1200 K for 2 hours increases the coercive force up to 6.3 kOe. The processes of crystallization from the amorphous phase, that improve the magnetic properties of barium ferrite, are discussed.

Keywords: Barium ferrite, plasma spraying, magnetic properties.

Highlights:

We studied the barium ferrite powdersafter plasma heating and rapid quenching.

We studied the processes of crystallization from the amorphous phase.

We studied theprocesses ofthermal annealing for the barium ferrite.

1. Introduction

Application of the amorphized and nanodispersed powders during the manufacture of ferrite products allows not only to intensify the sintering process, but also to control the ferrite microstructure. The directional crystallization during the transition from amorphous to crystalline state enables to control the amount of crystallization centers, the rate of nucleation

and growth of crystallites, the distribution and size of grains, the fraction and the ratio of crystalline phases, etc., thereby creating a certain microstructure of the material with the necessary set of physico-chemical properties [1-8].

Considering the possibility of amorphization, barium ferrite looks more preferable than spinel ferrites. This is because the binary oxide systems, which contain cations with greatly varied sizes, are easier to amorphize [9, 10]. In addition, barium ferrite has a more complex crystalline structure of magnetoplumbite (spatial group $D_{6h}^4 - Pb_3/mmc$). Its unit cell contains two formula units of $BaFe_{12}O_{19}$, and can be composed of sequential structural blocks S (with dense cubic packing of two layers of oxygen ions, characteristic forspinels) and R (with dense hexagonal packing of three oxygen layers). The sequential arrangementof hexagonal and cubic packings along the C axis leads to the formation of new (in comparison with spinel) nodes with fivefold coordination of (2b) position along with tetrahedral and octahedral nodes. Thus, cations $Fe_e^{3+}$are localized in crystallographically nonequivalent positions (2a, 2b, $4f_1$, $4f_2$, 12K). In this regard, let us consider the results of the investigation of the structural state and magnetic properties of barium ferrite sintered from rapidly quenched ferrite powders.

2. Materials and Methods

The phase composition of the obtained samples was analyzed using the Advance D8 X-ray diffractometer in CuK_α monochromatic radiation. The scanning was carried out at room temperature in the angular rangeof 30-120 deg in 2θwith a step of 0.04 deg.

The magnetic properties were studied by the method of vibrating magnetometry.

The thermographic studies were performed by the SETSYS Evolution equipment.

Mössbauer studies of the alloys were carried out at 78 K and 294 K by means ofnuclear gamma resonance spectrometer of electrodynamic type in a constant acceleration mode with ^{57}Co/Rh source. In order to calibrate the isomer shifts and speed scale, α-Fe foil was used at 294 K.

The morphological studies of the samples were performed by scanning microscopy (JEOL JSM-6490 LV).

The process equipment for plasma spraying and rapid quenching is discussed in detail in [11-20]. For the preparation of barium ferrite, rapidly quenched powders were used with the composition corresponding to the chemical composition of anisotropic magnets (Fe_2O_3–

84.1%, BaO–15.4%, additives of aluminum and boron oxide – not more than 0.5%). In order to achieve various cooling rates, the quenching of ferrite powders after plasma spraying was carried out in different medium: gaseous (in air), liquid (in water), and on the quenched copper disk. In all cases of quenching, the conditions for plasma spraying of powders were the same: a power of arc discharge of 18 kW, a medium of Ar/CO_2 gaseous mixture and a powder consumption of 14 g/min.

3. Results and discussion

The X-ray studies of the quenched samples showed that their crystal structure significantly changes (Fig. 1). It was found that, after quenching in the gaseous and liquid media, the barium ferrite powders become biphasic and they contain the basic phase of barium hexaferrite and small (~ 10%) inclusions of the cubic phase, which is expected to bethe phase of magnetite.

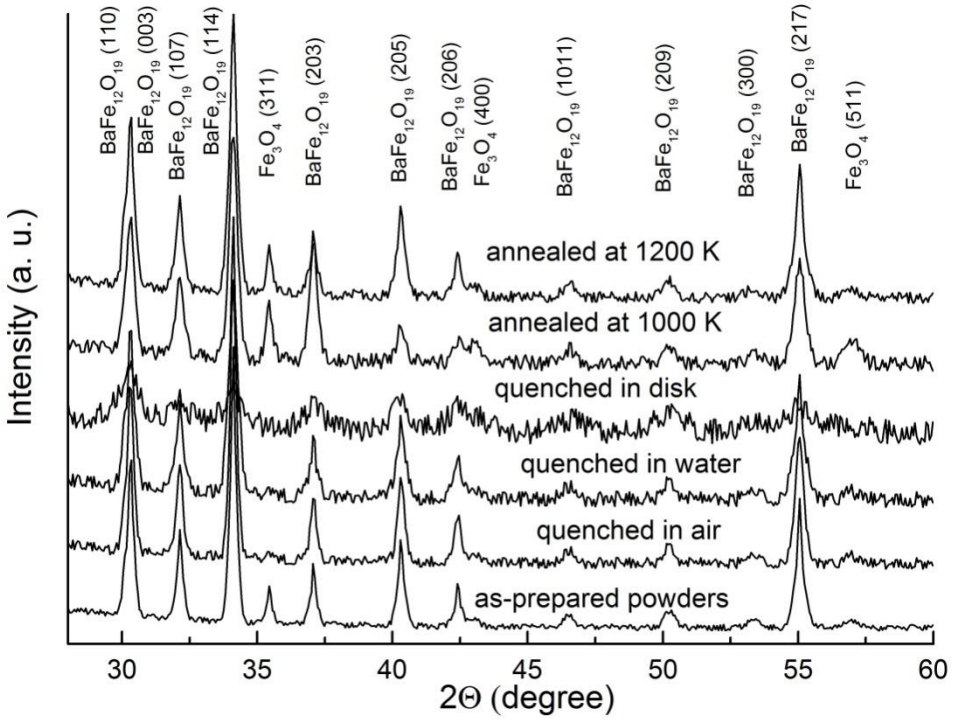

Fig 1. Diffraction pattern of barium ferrite: initial, quenched in various media (in air, in water, on the copper disk) and annealed at 1000 K and 1200 K for 2 hours

However, despite the savingof the basicphase, its structure was modified: a significant increase in the parameter *c* of the hexagonal unit cell was observed along with a practically

unchanged value of the parameter *a*. Such anisotropic "swelling" of a unit cell is most probably due to the formation of a vacancy in (2b) positions. Just in this case the oxygen octahedra of the hexagonal block is distorted and, consequently, the period of the unit cell increased. As for the selective formation of vacancies, it can be assumed that the states of Fe^{3+} ions localized in low-symmetry (2b) positions are energetically the least stable. Therefore the disordering defects arising during quenching are located predominantly in these positions.

The situation becomes different duringthe analysis of the structural state of samples quenched on the rotating copper disk. In this case, the X-ray diffraction spectra consist of a diffuse maximum observed in the small-angle region, which is characteristic of the amorphous state, and of broadened lines of low intensity corresponding to the cubic structure (Fig. 1). Consequently, as a result of rapid quenching, the initial hexagonal phase of ferrite completely disappears with the formation of new nonequilibrium cubic and amorphous phases. It is quite difficult to identify the cubic structure due to the diffuseness of the main diffraction peaks. It is most probably that the observed reflections of the cubic phase belong to the compounds Fe_3O_4 or γ-Fe_2O_3, which have similar lattice parameters and are therefore difficult to distinguish.

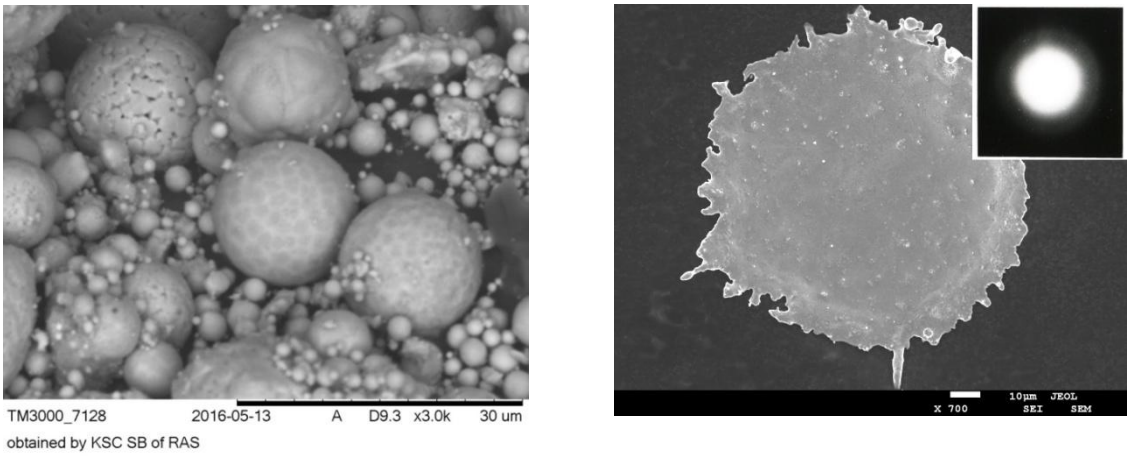

a b

Figure 2. Morphological pattern of Ba-ferrite powders quenched after plasma spraying: a - in air; b - on the surface of the copper disk (the inset shows the electron diffraction pattern of the thin section ~ 0.1 μm)

The morphological and electron diffraction analysis of the initial Ba-ferrite particles melted in the plasma and quenched in various media (Fig. 2) also testify the formation of

amorphous-crystalline state. When the powder was sprayed into a gas or liquid medium, the particles become near spherical. The process of shaping was accompanied by a change in the fractional composition of the powder, and the fragmentation of the particles into smaller ones was observed (the fraction of small particles with a size of <50 μm was equal to ~ 40%). The appearance of fine fraction can be associated with the destruction of the initial particles as a result of the heatstroke and gas-dynamic effects of the plasma jet. We should also note that crystallites with hexagonal structure are observed on the surface of large particles (Fig. 2a).

As a result of quenching the melt drops on the stationary metal copper plate (Fig. 2b), the particles had a luminary shape with a thickness of 0.1-2 microns and a diameter of 50-1000 microns. The investigations of the structural state obtained by the plasma splat quenching of Ba-ferrite showed that in the thinner sections of the flakes (<0.1 microns), the halo is observed on the electron diffraction patterns (Fig. 2b inset), which indicates the achievement of amorphous state.

In order to clarify the phase composition of the quenched samples, they were investigated by the method of NGR spectroscopy. Fig. 3 shows the γ-spectrum of the barium ferrite sample that was quenched on the copper disk after plasma spraying.

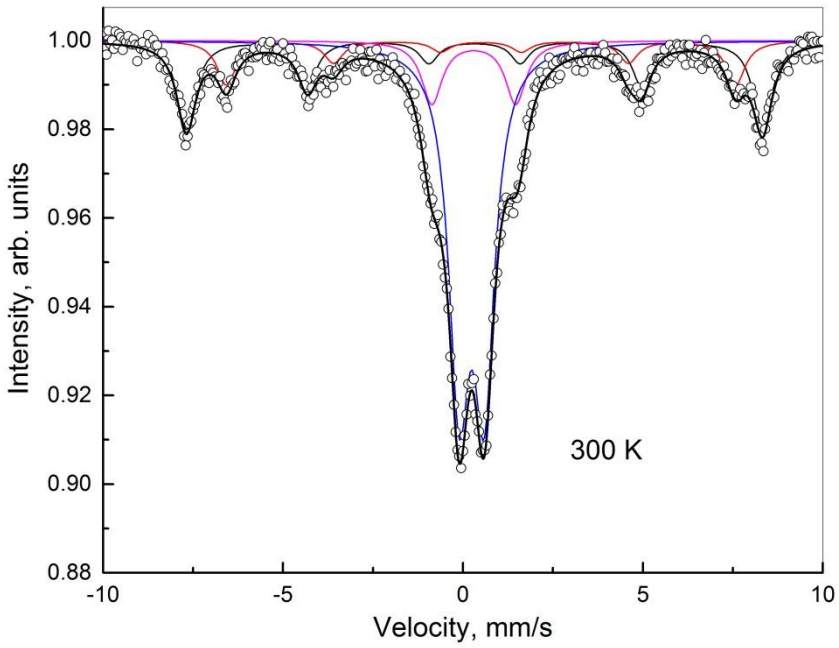

Fig 3. Mössbauer spectrum of the barium ferrite sample after plasma treatment and quenching on the disk

The spectral processing was carried out simultaneouslyby model interpretation of the quadrupole doublet and recovery of the hyperfine magnetic field distribution. The Mossbauer spectrum represents a superposition of the intense doublet located in the central part, a low-intensity doublet and two low-intensity sextets, characteristic of superparamagnetic particles. The intense doublet with the average parameters <IS> = 0.24 mm/s and <QS> = 0.71 mm/s corresponds to the positions of trivalent iron atoms in the tetrahedral surrounding environment of oxygen atoms. And the doublet of low intensity with the average parameters <IS> = 0.27 mm/s and <QS> = 2.33 mm/s corresponds to the positions of bivalent iron atoms. The areaof sextuplets was used to estimate the fraction of magnetite in the total amount of the crystalline phase, which was found to be ~ 5%.

We should also note that crystalline compounds, which include barium, were not found. Therefore, it can be assumed that Ba ions are in the amorphous phase.

Nonequilibrium state arising during quenching of barium ferrites is also shown by thermographic studies. The DTA curves of the quenched samples are characterized by two peaks of heat release: in the region corresponding to 620-820 K and at T = 1153 K (Fig. 4a).

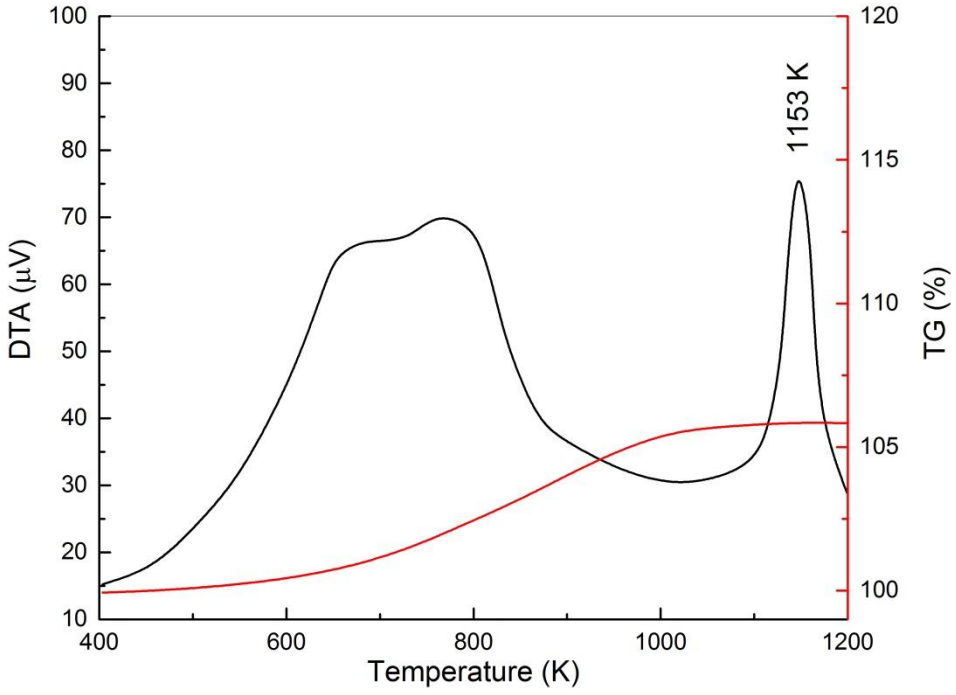

a)

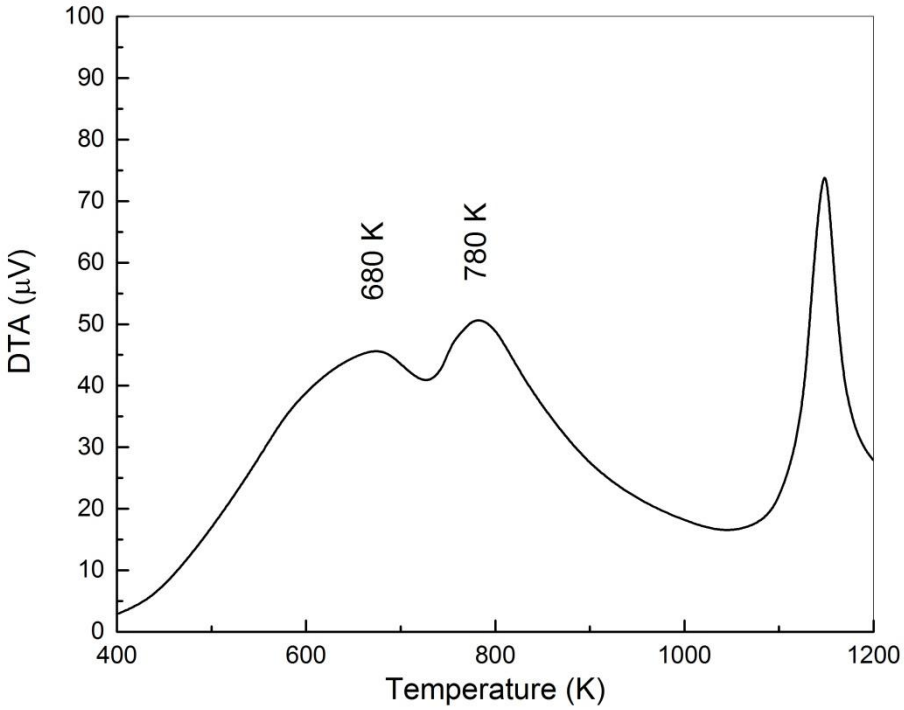

b)

Figure 4. Thermograms of the barium ferrite quenched on the disk: a) in air, b) in argon

The wide low-temperature maximum is clearly defined for the oxidizing medium, and the heat release process is accompanied by an increase in the weight of the sample. This suggests that oxidation processes of ferrite powders, partially reduced during plasma spraying, occur in this temperature range. The intensity and position of the narrow high-temperature maximum are practically independent of the composition of the gaseous medium and, apparently, its appearance is due to crystallization of the amorphous phase.

In an inert medium, the intensity of the low-temperature maximum significantly decreases, and the change in weight is practically not observed. The DTA curves clearly show two characteristic temperature regions of exothermic reactions, confirming the nonequilibrium state of the studied samples. In the region corresponding to 780 K, thereactions of cation redistribution occur and the statistical distribution of cations returns to the initial thermodynamically equilibrium distribution. The low-temperature maximumof DTA (680 K) is observed in a wider temperature region and can be related both to relaxation of local stresses and to the redistribution of cations over the nonequivalent positions of a separate sublattice.

In order to study the character of the transformations occurring during heating, the quenched samples were successively annealed for two hours at the temperatures of 500–1500 K. After each annealing, diffraction patterns were taken and the differential thermal analysis of the powders was carried out.

Annealing of the samples at the temperatures of up to 900 K leads to amore clearrevealing of the reflexes of the cubic structure and the appearance of additional diffraction peaks corresponding to the α-Fe_2O_3 phase. Such changes can take place both due to the oxidation of magnetite, and as a result of the following transformation:γ-Fe_2O_3 → α-Fe_2O_3.

The most significant changes in the diffraction spectrum were observed at the samples exposed to the thermal annealing in the temperature range of 960-1100 K. In this case, reflexes of the hexagonal phase of $BaFe_{12}O_{19}$ appear and become possible, while the intensity of the abovementioned reflections of the cubic phase decreases by more than an order of magnitude (Fig. 1). Simultaneously, the intensity of the high-temperature peak (the DTA thermograph), that characterizes the crystallization process of the amorphous phase, decreases.

At the annealing temperature T = 1173 K, the phase transformations are mainly completed and the final formation of the microstructure of barium hexaferrite occurs (Fig. 1). We should note that in this case the structure of hexafferrite $BaFe_{12}O_{19}$ is formed without intermediate stages of the formation of various modifications of $BaFe_2O_4$monoferrite, which usually does not occur under the conditions of the equilibrium ferrite synthesis.

The structural and phase changes, occurring in the quenched samples of barium ferrite,must definitely change the magnetic properties. Table 1 shows the most practically important characteristics of the demagnetization curve: a coercive force H_c and saturation magnetization σ_s.

Below are the results of investigations, in which Ba-ferrite nanoparticles were produced by various methods [21-23].

Table 1. Magnetic properties of barium ferrite samples

Quenching conditions	σ_s, emu/g	H_c, Oe
Initial sample	66	3500
Quenching in water	57	920
Quenching on the disk	44	340
After annealing at 1260 K	64,2	6320

In the work [23]	60,75	5691
In the work [22]	65,8	5251
In the work [21]	64,3	5483,3

It can be seen that with an increase in the quenching rate (due to spraying in various media), the hysteresis curves are significantly transformed. The most significant changes in the magnetic parameters (the decrease of a coercive force by one order and a magnetization by almost twice) are observed in the case of quenching barium ferrite on the copper disk. That is, it takes place when radical structural transformations occur in the material and the amorphous phase forms.

The behavior of the magnetic properties (H_c, σ_s) during isochronous annealing of quenched samples is shown in Fig. 5.

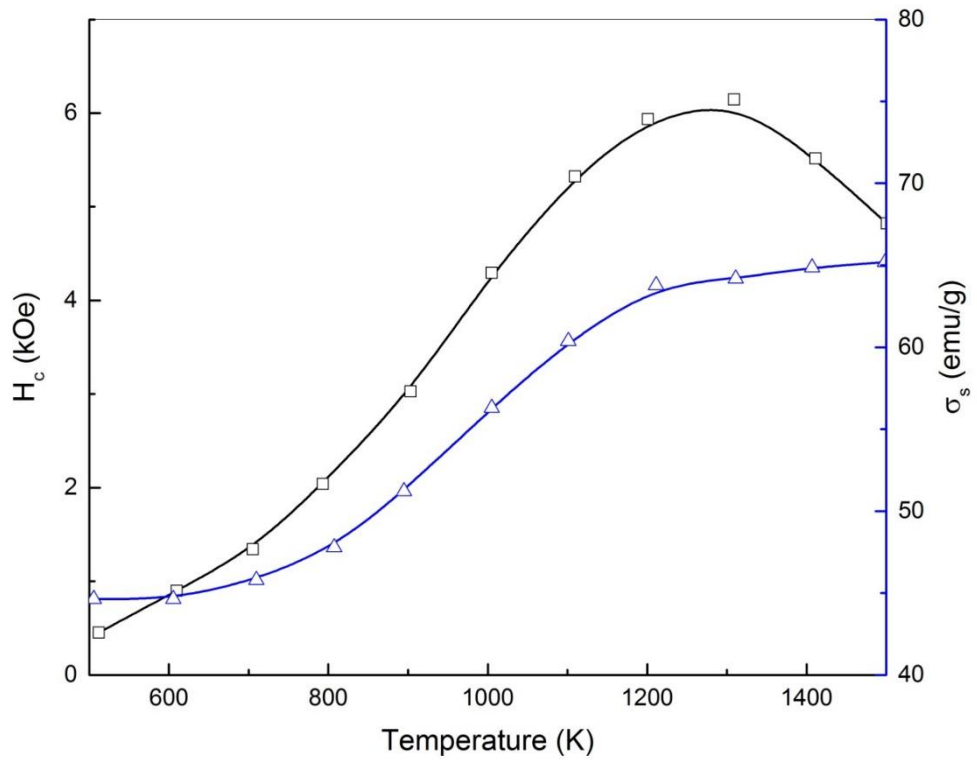

Fig. 5. Dependences of the coercive force H_c and the saturation magnetization σ_s on the temperature of isochronous annealing

It is obvious that during the process of thermal annealing, it is possible not only to recover the magnetic parameters of the barium ferrite, but also significantly improve them. The recovering of the saturation magnetization σ_s occurs during one stage, and this process

goes most intensive in the temperature range corresponding to the formation of the hexagonal phase.

The coercive force H_C has the different dependence on the annealing temperature. An increase in the coercive force is observed in the temperature range of up to T = 1260 °C, where it reaches its maximum value. This value was higher for such the samples of barium ferrite, which had higher quenching rate. Thus, in the case of quenching ferrite in water, the maximum value of the coercive force does not exceed the initial level. While in the case of the quenching on the copper disk, the maximum value of the $H_c$during the thermal annealing wasfound to be 6300 Oe, that is almost twice higher than the coercive force of the initial material. A further increase in the annealing temperature leads to a decrease in the coercive force, so that even at T_{ann} = 1600 K, the H_C decreases to the initial level.

The obtained results proof the significant role of the prehistory (structural disordering and phase composition) of the initial powders in the formation of the high-coercive state of the barium ferrite. Since only one phase (barium hexaferrite) is formed during the sintering process (T= 1200 K) of all types of quenched powders, hereby the observed differences in the magnetic properties can be related to the peculiarities of the microstructure, which, for example, in the case of quenching ferrite on the disk, is formed both under the conditions of polymorphic transformation and in the process of crystallization of the amorphous phase.

A detailed analysis of the macrostructure of the quenched and sintered powders of barium ferrite revealed the following. After plasma spraying and quenching on the copper disk, the ferrite passes into a strongly nonequilibrium state, characteristic of glassceramic, where small crystalline inclusions of the compounds Fe_3O_4 and γ-$Fe_2O_3$with average size of 0.05-0.08 μm present in the amorphous matrix.

During thermal annealing, beginning at T = 950 K, a magnetically ordered nano-crystalline hexagonal phase of $BaFe_{12}O_{19}$ is formed. The size of crystallites in thenew phase depends on the temperature and duration of annealing. At T = 1260 K and t = 2 h, that is, under such sintering conditions, when the coercive force becomes maximum, the crystallites reach 0.1 μm in size (Figure 6).

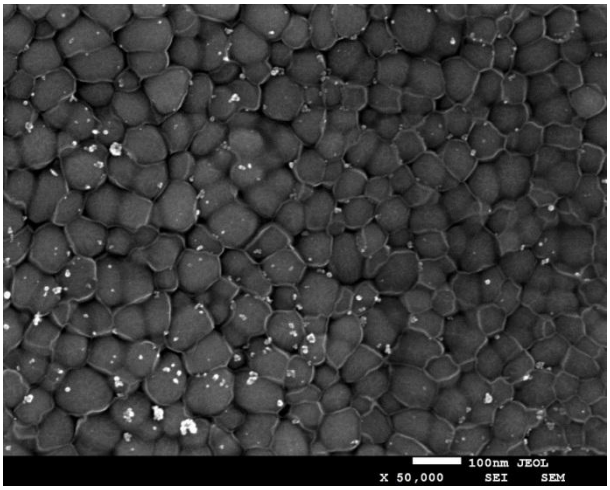

Fig. 6. Microstructure of barium ferrite after quenching on the disk and subsequent annealing at 1200 K for 2 hours

Apparently, these values are optimal for the realization of the high-coercive state of the barium ferrite. A further increase in the annealing temperature leads to an increase ofa size of the crystalline grains and a decrease of the coercive force.

Conclusion

Thus, applying the traditional methods of powder metallurgy and combining the sintering process with the transition from amorphous to crystalline state, it is possible to produce barium ferrites with high performance characteristics. A similar application of the transition from amorphous to crystalline state for the formation of the properties of metallic alloys important for practical applications, was reported in. In this regard, the obtained results confirm the opinion that the application of amorphous powders for producing materials with the necessary microstructure is one of the advanced directions in the technology of powder metallurgy.

Acknowledgements

The reported study was funded by Russian Foundation for Basic Research, Government of Krasnoyarsk Territory, Krasnoyarsk Region Science and Technology Support Fund to the research projects No 17-48-240806 and No 01/17.

References

1 González J, Zhukov A2006Amorphous magnetic materials for sensors.Book: Encyclopedia of Sensors. American Scientific Publishers. **1**79-103.

2 Chiriac H, Ovari T A1996 Amorphous glass-covered magnetic wires: preparation, properties, applications*Progress in Material Science*. **40**333-407.doi.org/10.1016/S0079-6425(97)00001-7.

3 Awawdeh M, Bsoul I, Mahmood SH 2014Magnetic properties and Mossbauer spectroscopy on Ga, Al, and Cr substituted hexaferrites *J Alloys Compd* **585** 465–473. doi:10.1016/j.jallcom.2013.09.174.

4 Lepeshev A.A., Rozhkova E.A., Karpov I.V., Ushakov A.V., Fedorov L.Y. Physical, mechanical, and tribological properties of quasicrystalline al-cu-fe coatings prepared by plasma spraying // Physics of the Solid State. 2013. T. 55. № 12. C. 2531-2536.

5 Afghahi S, Jafarian M, Salehi M, Atassi Y 2017 Improvement of the performance of microwave X band absorbers based on pure and doped Ba-hexaferrite *J Magn Magn Mater***421** 340-348. doi:10.1016/j.jmmm.2016.08.042.

6 Guner S, Auwal IA, Baykal A, Sozeri H 2016 Synthesis, characterization and magnetooptical properties of $BaBi_xLa_xY_xFe_{12-3x}O_{19}$ ($0.0 \leq x \leq 0.33$) hexaferrites *J Magn Magn Mater***416**, 261–268. doi:10.1016/j.jmmm.2016.04.091.

7 Mosleh Z, Kameli P, Poorbaferani A, Ranjbar M, Salamati H 2016Structural, magnetic and microwave absorption properties of Ce-doped barium hexaferrite *J Magn Magn Mater***397** 101–107. doi:10.1016/j.jmmm.2015.08.078.

8 Alama RS, Moradia M, Rostamia M, Nikmanesh H, Moayedi R, Bai Y 2015 Structural, magnetic and microwave absorption properties of doped Ba-hexaferrite nanoparticles synthesized by co-precipitation method *J Magn Magn Mater***381** 1–9. doi:10.1016/j.jmmm.2014.12.059.

9Inoue A, Makino A, Mizushima T2000Ferromagnetic bulk glassy alloy *J Magn and Magn Mater*.**215–216**246-252.https://doi.org/10.1016/S0304-8853(00)00127-X.

10 Tones H 1973Splat cooling and metastable phases*Rep Proc Phys***36**1425–1497.

11 Ushakov AV, Karpov IV, Lepeshev AA, Petrov MI and FedorovLYu 2015 Specific features of the behavior of electroarcCuOnanoparticles in a magnetic field *Phys. Solid State* **57** 919–923.doi: 10.1134/S1063783415050303.

12 Lepeshev AA, Bayukov OA, Rozhkova EA, Karpov IV, Ushakov AV and FedorovLYu 2015 Modification of the phase state andstructure of the Al–Cu–Fe quasi-

crystalline alloy during plasma deposition *Phys. Solid State.* **57** 255–259. doi: 10.1007/s10876-011-0378-2.

13 Lepeshev AA, Karpov IV, Ushakov AV and Nagibin GE 2016 The morphological and structural features of ferrite compositions$(1-x)MeFe_2O_4 \cdot xP_2O_5$ prepared by plasma spraying *J. Alloys Compd.* **663** 631–635.doi:10.1016/j.jallcom.2015.12.168.

14 Lepeshev, Ushakov A.V., Karpov I.V. Low-temperature magnetic behavior of nanostructured ferrite compositions prepared by plasma spraying // Journal of Applied Physics. – 2017. – Vol. 122, No. 10, p. 104103. doi: 10.1063/1.5001506.

15 Ushakov AV, Karpov IV, Lepeshev AA,ZharkovSM 2016The influence of oxygen concentration on the formation of CuO and Cu_2O crystalline phases during the synthesis in the plasma of low pressure arc discharge *Vacuum***128** 123-127. doi: 10.1016/j.vacuum.2016.03.025.

16 Ushakov AV, Karpov IV, Lepeshev AA, Petrov MI 2016Plasma-chemical synthesis of copper oxide nanoparticles in a low-pressure arc discharge*Vacuum***133**25-30. doi: 10.1016/j.vacuum.2016.08.007.

17 Ushakov AV, Karpov IV, LepeshevAA 2017Plasma-chemical synthesis of Fe_3O_4 nanoparticles for doping of high-temperature superconductors *J of Superconductivity and Novel Magnetism***30** 311-316. doi:10.1007/s10948-016-3709-6.

18 LepeshevAA, KarpovIV, UshakovAV, NagibinGE 2017 Magnetic and resonant properties of ferrite compositions $(1-x)$ $MeFe_2O_4 \cdot xP_2O_5$ prepared by plasma spraying*Materials Research Express***4** 056101. doi: https://doi.org/10.1088/2053-1591/aa6c81.

19 LepeshevAA, UshakovAV, KarpovIV, BalaevDA, KrasikovAA, DubrovskiyAA, VelikanovDA, Petrov MI 2017Particularities of the magnetic state of CuO nanoparticles produced by low-pressure plasma arc discharge *J of Superconductivity and Novel Magnetism***30** 931-936. doi:10.1007/s10948-016-3885-4.

20 Ushakov AV, Karpov IV, Lepeshev AA 2016Influence of the Oxygen Concentration on the Formation of Crystalline Phases of TiO_2 during the Low-Pressure Arc-Discharge Plasma Synthesis*Technical Physics***61** 260-264. doi: 10.1134/S1063784216020262.

21 Xu P, Han X, Wang M Synthesis and Magnetic Properties of $BaFe_{12}O_{19}$ Hexaferrite Nanoparticles by a Reverse Microemulsion Technique *J. Phys. Chem. C***111** 5866–5870. doi: 10.1021/jp068955c.

22 Yu J, TangS, Zhai L, ShiY, Du YSynthesis and magnetic properties of single-crystalline $BaFe_{12}O_{19}$ nanoparticles*Physica B: Condensed Matter***404** 4253-4256. https://doi.org/10.1016/j.physb.2009.08.043.

23 LiY, Wang Q, Yang HSynthesis, characterization and magnetic properties on nanocrystalline $BaFe_{12}O_{19}$ ferrite *Current Applied Physics***9** 1375-1380. https://doi.org/10.1016/j.cap.2009.03.002.